

THS 27415356.





This is to certify that the

thesis entitled

MELTWATER DRAINAGE FROM TEMPERATE GLACIAL ICE BURROUGHS GLACIER SOUTHEAST ALASKA

presented by

Ryan Jay Simmons

has been accepted towards fulfillment of the requirements for

M.S. degree in Geology

Qualam James
Major professor

Date 4 May 1989

O-7639

MSU is an Affirmative Action/Equal Opportunity Institution

PLACE IN RETURN BOX to remove this checkout from your record. TO AVOID FINES return on or before date due.

DATE DUE	DATE DUE	DATE DUE

MSU Is An Affirmative Action/Equal Opportunity Institution

MELTWATER DRAINAGE FROM TEMPERATE GLACIAL ICE BURROUGHS GLACIER SOUTHEAST ALASKA

Ву

Ryan Jay Simmons

A THESIS

Submitted to
Michigan State University
in partial fulfillment of the requirements
for the degree of

MASTER OF SCIENCE

Department of Geological Sciences

1989

ABSTRACT

MELTWATER DRAINAGE FROM TEMPERATE GLACIAL ICE BURROUGHS GLACIER SOUTHEAST ALASKA

By

Ryan Jay Simmons

A surface runoff model was applied to a temperate glacier in southeast Alaska in order to determine the method of meltwater drainage from unweathered glacial ice. Melt input for the model was calculated, for points on a north-south grid over the glacier surface, over a period of four sunny days in August 1973. The melt was then applied to a Route-and-Lag runoff model to create discharge hydrographs for the glacier for the duration of the study period. The resultant model discharges were then compared to actual drainage hydrographs for the same four day period. As a result of this comparison, it was determined that meltwater drainage from the glacier is predominantly through surface runoff.

ACKNOWLEDGEMENTS

I would like to extend thanks to my thesis advisor, Dr. Grahame Larson, for his guidance and extreme patience. The members of my thesis committee, Dr. David Long and Dr. Larry Segerlind, also deserve mention for their cooperation. My parents, Robert and Rose Simmons, perhaps deserve the greatest credit of all for their support, and encouragement.

TABLE OF CONTENTS

List of Tables	v
List of Figures	v i
I. Introduction	_1
	3
Basin Hydrology	3
	5
Glacial Characteristics	6
	8
IV. Runoff1	1 1
V. Results2	2 4
VI. Conclusions 2	28
Appendix A. Ice Melt Calculations 3	3 1
	3 7
Appendix C. Program for Calculating Hour Angles4	4 2
Appendix D. Program for Calculating Radiation Receipts and Melt	4 3
Appendix E. Program for Calculating Lumped Lagged Flow4	4 4
Appendix F. Program for Calculating Distributed Lagged Flow_4	48
Appendix G. Program for Routing Flow	50
	5 1

LIST OF TABLES

1	Basin Lag Values	1 4
2	Maximum Values of t for each Basin of	
	Burroughs Glacier	1 7
3	Basin Conversion Constants for Travel Time	1 8
4	Total Stream Discharge during the Study	2 5
5	Daily Variable Data Values	3 7

LIST OF FIGURES

1	Subbasins of Burroughs Glacier	4
2	Radiation Receipts and Melt through Time	1 0
3	Surface Runoff Flow Lines Burroughs Glacier	1 5
4	Absolute Travel Time Isochrone Map Burroughs Glacier	r_19
5	Lumped Model Lagged Hydrographs	20
6	Distributed Model Lagged Hydrographs	2 1
7	Lumped vs. Distributed Model Outputs	22
8	Routed Hydrographs vs. Actual Hydrographs	23
9	Surface Slope Burroughs Glacier	39
10_	Surface Azimuth Burroughs Glacier	40
11_	Surface Albedo Burroughs Glacier	4 1

I. Introduction

According to Drewry (1986), there are six main sources of liquid water in temperate glaciers. These include: surface ice melt; ice melt due to mechanical stress and strain; ice melt from geothermal heating; groundwater flow; surface runoff; and, liquid precipitation. This water may be found on top of, within, under, and adjacent to the glacial ice. Surface (supraglacial) water is usually drained via running streams (Drewry, 1986) which may discharge into tubes, or moulins, which pierce the glacier surface and connect to a system of tubular conduits branching through the body of the glacier and converging at a single discharge point at the glacier terminus. Water within the glacial ice itself (englacial water) can drain through a system of intergranular veins and capillaries between the ice crystals (Nye, 1976; Nye and Frank, 1973). Liquid water at the base of a glacier may also drain as a thin film spread uniformly between the ice and bedrock (Nye, 1973; Freeze, 1972).

In this study, meltwater production and surface runoff associated with Burroughs Glacier, in southeast Alaska, is modeled for a period of four days using solar radiation receipts and a timearea lag-and-route method. The purpose for modeling the melt and runoff is to determine if surface runoff alone can account for most of

the meltwater emanating from the glacier margin during periods of high meltwater production.

Burroughs Glacier was chosen for the investigation because it is hydrologically a very simple system to model. It lies completely below the equilibrium line so that at the height of summer there is no snow remaining on the glacier surface to absorb meltwater or complicate the drainage. Also, since the glacier is temperate and at the pressure melting point throughout, no meltwater is removed from storage through refreezing. The glacier is drained by well defined streams whose channels are generally stable and suitable for monitoring of stream discharge.

Another reason for choosing Burroughs glacier is the availability of usable data. Many meteorological, glacial, and geological studies have been made in the general area surrounding Burroughs glacier. One such study, conducted by G. Larson in the summer of 1973, provides all the necessary data for testing a runoff model such as will be used in this study. Larson's meteorological data can be used to calculate melt - which can be applied to a surface runoff model. Moreover, discharge data, from streams draining Burroughs glacier for this period, can be used as a means of judging model accuracy.

II. BACKGROUND INFORMATION

Burroughs Glacier is a small body of stagnant ice roughly 13 km long and 1.2 to 3 km wide. It is located just north of Wachusett Inlet, about 120 km northwest of Juneau (59' 00" North Latitude, 136' 20" Longitude), and is one in a series of hundreds of small ice bodies within the northeast corner of Glacier Bay National Monument. Two tongues of ice, flowing in two different directions from an ice divide, compose the body of the glacier.

Basin Hydrology

Early records from the late 1800's show that Burroughs glacier was once part of a much larger body of ice, the Cushing Plateau (Mickelson, 1971). The ice at that time was around 850 m high in the Burroughs glacier area. Over the years, however, it has melted at a rate of as much as 8 m/year and has resulted in a gradual reduction in glacier size until all that remains today are a number of small individual glaciers occupying valley basins.

This study concentrates upon the eastern tongue of Burroughs Glacier which lies within an east-west striking basin 27.2 square kilometers in area (see figure 1). The tongue is 6.8 km long, 2.2 to 3 km wide, and 13.9 square kilometers in area, and is bounded to the

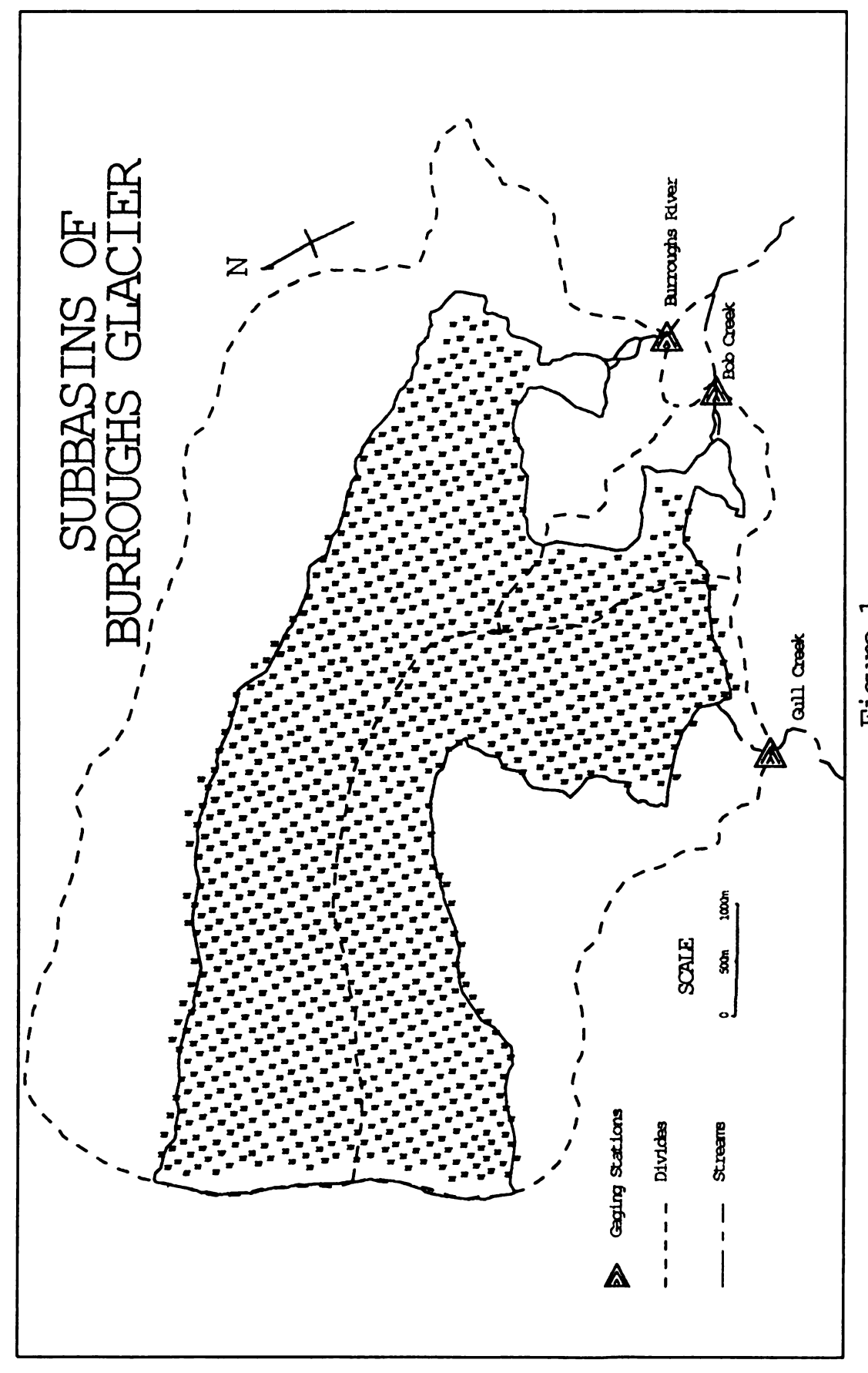


Figure 1

north by Minnesota Ridge and to the east by the Curtis Hills and to the south by the Bruce Hills. It is also cut off from all other ice bodies by the encircling mountain ridges so that no ice is added to the basin from outside sources. The ice divide separating the eastern tongue from the western tongue is also at such a low elevation that the ice is entirely below the equilibrium line (Larson, 1978). As such, the yearly snow input on the glacier surface completely melts each summer - allowing no buildup of snow to produce new glacial ice. Moreover, not only does each years snow melt off, but some of the glacial ice melts along with it.

Since the eastern tongue of Burroughs Glacier is surrounded by mountains, surface water flow is blocked from entering from outside the basin. The crystalline bedrock of the basin also does not allow for any major exchange between groundwater and surfacewater. Thus, the eastern tongue of Burroughs Glacier may be considered an isolated system, such that any water exiting the glacier must be derived from the glacier itself or from precipitation falling within the basin.

Climate and Physical Setting

The general climate in the vicinity of Burroughs Glacier has been described by Loewe (1966) and McKenzie (1968, 1970). Due to the proximity of the pacific coastal waters, the climate may be characterized as maritime. No permanent meteorological stations have been located on the glacier itself, however, meteorological measurements have been taken during numerous expeditions since

the year 1959 (Taylor, 1962; Mickelson, 1971; Larson, 1977 & 1978). Records of these measurements show: an average temperature of $10^{\circ}\text{C} \pm 5^{\circ}$; rainfall of 200 mm/month; and, mostly overcast conditions.

The bedrock beneath and around Burroughs Glacier consists of metamorphosed shales and limestones intruded by diorite and granodiorite stocks. The metasediments are of paleozoic age and generally occupy the eastern half of the basin. Moreover, the stocks are of cretaceous age and occupy the western half of the basin. In scattered areas, unconsolidated sediments mantle the bedrock and consist of sandy till along with well-sorted sand and gravel. The till ranges in thickness from a thin 'veneer' to more than 25 meters in some places. The sand and gravel exist mostly in kame terraces near valley walls.

On the basis of dye tracer experiments Larson (1978) was able to divide the eastern tongue of Burroughs Glacier into three subbasins for drainage purposes (see figure 1). Each of these subbasins is drained by its own stream: basin 1 by Burroughs River; basin 2 by Bob Creek; and, basin 3 by Gull Creek.

Glacier Characteristics

The surface texture of Burroughs Glacier varies greatly. Near the glacier terminus, for example, ice crystals are generally coarse and equigranular and range from five to ten centimeters in diameter (Larson, 1978). They sometimes appear slightly melted at their boundaries so that they are often loose, which gives the surface a

disintegrated appearance. Further away from the terminus, however, the ice is fine grained, foliated, and does not have a disintegrated appearance. Also, individual crystals are irregularly shaped and are generally less than two centimeters in diameter.

The glacial surface is also characterized by several types of structures (Taylor, 1962). These include foliation, banding, fractures and crevasses. The foliation consists of parallel bands of bubble-free and bubble-rich ice running parallel to Minnesota Ridge. The banding consists of horizontal layering caused by a differential fine-sediment content of the ice. Most of the fractures and crevasses on the glacier surface are vertical, less than 30 cm wide, and as much as 10 meters deep. At higher elevations, they form a transverse system while, in lower regions, they are more longitudinal.

III. MELT

Larson (1978) found that short-wave global radiation is the dominate energy source for melt on Burroughs Glacier during clear sunny days. He also found that other sources of energy (such as net long-wave radiation, convective heat transfer, and conductive heat transfer) generally balance each other out, and that short-wave radiation alone could be used to approximate melt at a single point anywhere on the glacier surface.

For this reason, it was decided to use a cloudless four day period to estimate melt on the glacier surface. This was done by placing a north-south rectangular grid of 70 x 60 points over the glacier (see figure 1) and calculating radiation receipts at each such point. In order to account for melt variation through time energy receipts were repeatedly calculated for each point at specified time intervals. Melt was calculated for each point by multiplying radiation receipts by a conversion constant (the latent heat of fusion).

Melt was calculated, at a specified times for each grid point, using a computer program based on radiation equations developed by Kondratyev (1969). Inputs to the routine include: time of sunrise; time of sunset; declination; transimissivity; radius vector; albedo;

surface slope; and surface slope azimuth (see Appendix A). The program applies the radiation equation to each grid point for each half hour interval, for all four days of the period August 14 to August 17, 1973, starting with the half hour immediately preceding dawn and ending with the half hour immediately following dusk. The total radiation received, and volume of melt, over the entire surface for each day of the study, as well as the sum for the whole four day period, was also calculated.

Figure 2 shows the variation in solar radiation receipts over the basin surface, and the rate of meltwater production, through time. On the figures, four peaked curves represent the radiation influx to the surface during the four days. Solar radiation seems to be at a maximum during solar noon of each day, decreasing with time on either side of the peak until dawn or dusk is reached. Energy inputs between dusk and dawn are zero. A comparison of radiation receipts and melt shows that when there is a maximum of radiation at the surface there is a maximum melt and when there is a minimum of radiation inputted to the surface there is a minimum melt.

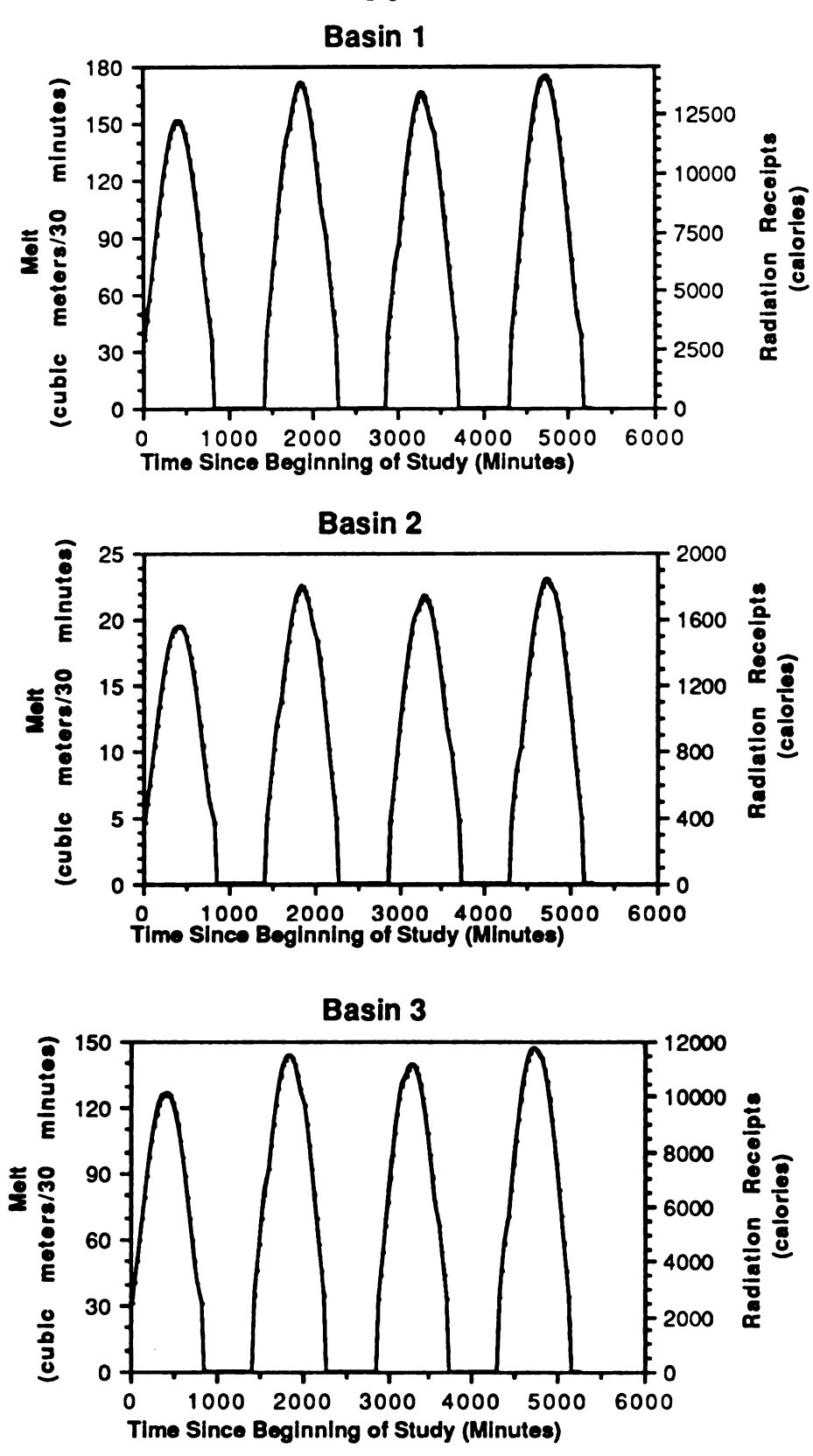


Figure 2. Radiation Receipts and Melt through Time

IV. RUNOFF

The lag-and-route method (Laurenson, 1964; Raudkivi, 1979) was used to model meltwater runoff over the surface of Burroughs Glacier. This method calculates the effects of both the translatory (lagged) and storage (routed) movement of meltwater for each subbasin of Burroughs Glacier.

The lag method was applied in two ways. In the first application of the lag method, the subbasins were divided into "lumped" zones and the sum of the runoff from each such zone was calculated. In the second application of the lag method, flow from specified points "distributed" over the drainage basin was calculated - seemingly more representative of areal variations in slope and melt. The first method, the "lumped" lagging method, was developed to minimize the number of necessary calculations; however, the second method, the "distributed" lagging method, seems to lend itself more readily to computer application - a matter of applying a set of flow equations to each grid point.

For the lumped lagging method, inflow (in the form of meltwater production) was lagged by dividing each subbasin into a number of zones by isochrones of runoff travel time to the subbasin outlets. The area between isochrones was calculated and was assigned an average travel time (taken as the average of the two

isochrones defining the zone). The contour interval between isochrones was chosen as the duration of the inflow (meltwater production) increment for ease of computation (Linsley, Kohler &Paulus 1975). The inflow was then lagged by determining the inflow value between isochrones and calculating an average discharge for each isochrone zone by the equation:

Q = PA/T

where:

Q = discharge from the zone in question

P = average melt for the zone

A = area of the zone

T = time increment of precipitation = time between zone isochrones

A lagged discharge hydrograph, for each inflow increment, was produced by calculating the discharge ordinate for each time increment as follows:

$$I_n = P_n A_1 + P_{n-1} A_2 + \dots + P_1 A_n$$

where:

I_n = lagged hydrograph ordinate at time n

P_n= inflow (melt) at time n

 A_n = area between the (n-1) and the n-th isochrone

n = number of subzones

The lagged hydrograph for each event was then added together to produce a compound lagged discharge hydrograph. See Appendix E for the computer routine written to calculate the lagged flow in this manner.

For the distributed lagging method flow was calculated for each point on the glacier surface. Runoff travel times were calculated for each grid point on the glacier. Melt, calculated for each grid point, was then added to a total compound basin hydrograph according to the time that it took that melt to reach the basin outlet (the runoff travel time). See Appendix F for the computer routine written to calculate the lagged flow in this manner.

The lagged discharge hydrograph was routed through storage to get the actual hydrograph for each subbasin. Routing was accomplished through the use of the Muskingum storage routine, as outlined by Laurenson (1964) and Raudkivi (1972). This routine assumes outflow at any time depends upon both preceding outflow and preceding inflow and is expressed as follows:

$$O_n = C_0 I_n + C_1 I_{n-1} + C_2 O_{n-1}$$

where:

O = routed discharge ordinate

I = lagged discharge ordinate = inflow ordinate for route model

$$C_0 = \frac{0.5t}{k + 0.5t}$$

$$C_1 = C_0$$

$$C_2 = \frac{k - 0.5t}{k + 0.5t}$$

t = routing period

k = storage constant

In the above equation, the storage constant is the ratio of storage to discharge. According to Linsley, Kohler and Paulhus (1975), k is approximately equal to the travel time through the reach through which the method is being applied and may be equated to the average travel time for the basin (which is the basin lag).

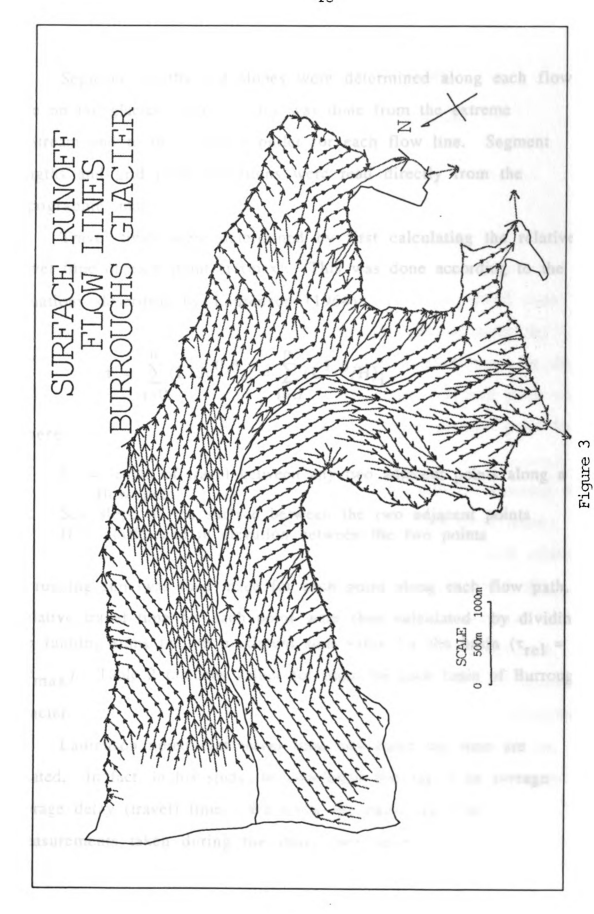
The computer routine developed to perform the task of routing flow is shown in Appendix G. Input to this routine included tabular files containing the lagged hydrograph ordinates for each half-hour time increment, the time increment for routing (one half-hour), and the storage constant (basin lag) for each basin of Burroughs Glacier (see table 1 for basin lag values).

Table 1. Basin Lag Values

	Basin Lag
Basin	(hours)
1	3.22
2	3.05
3	3.21

APPLICATION

The grid points used to calculate melt in chapter 3 were used in the calculation of flow lines. These points were superimposed on a topographic map of the area and flow lines were drawn between them based on slope direction. Figure 3 shows the flow lines drawn for subbasins 1, 2, and 3.



Segment lengths and slopes were determined along each flow line on the glacier surface. This was done from the extreme upstream end to the subbasin outlet for each flow line. Segment lengths and grid point elevations were read directly from the topographic maps.

Travel times were determined by first calculating the relative travel time of each point $(\tau/\tau max)$. This was done according to the equations described by Laurenson (1964):

$$\tau = \sum_{i=0}^{n} (L/Sc^{0.5})_i = \sum_{i=0}^{n} (L^{1.5}/H)_i$$

where:

L = length of travel between any two adjacent points along a flow path

Sc= slope of the surface between the two adjacent points H = difference in elevation between the two points

A running sum was then made for each point along each flow path. Relative travel time for each point were then calculated by dividing the running sums by the maximum sum value for the basin ($\tau_{rel} = \tau/\tau_{max}$). Table 2 includes values for tmax for each basin of Burroughs Glacier.

Laurenson noted that travel time and basin lag time are related. In fact, in his study, he concluded that lag is an average storage delay (travel) time. We know the basin lag from measurements taken during the study (see table 1).

Table 2. Maximum Values of τ for each Basin of Burroughs Glacier

Basin	Relative Travel Time (τ)
1	26922
2	3482
3	17539

Assuming a linear relationship between relative travel time and absolute (i.e. k(tr)=k(ta)), a basin constant was calculated by dividing the absolute travel time by the relative travel time for the point. Absolute travel times were then calculated for each point on the surface by multiplying the relative travel time at each point by the basin constant.

In his study, Laurenson equated basin lag with the centroid of the time-area diagram. This could be taken as a weighted mean (with the weight factor being the area corresponding to each relative travel time value). Applying this to Burroughs Glacier, with the weighted mean being calculated for the relative travel time at each nodal point on the surface (with the weight factor being the area surrounding each point), the centroid for each subbasin was located. Because this "centroid" corresponds to basin lag, the basin conversion constant could be calculated from travel time values at this point. The basin conversion constants for basins 1, 2, and 3 are shown in table 3.

Table 3. Basin Conversion Constants for Travel Time

Basin	Mean τ	Conversion Constant (hours)
1	0.610	5 270
1	0.610	5.279
2	0.520	5.865
3	0.460	6.978

The relative travel time value at each point was multiplied by the conversion constant for each subbasin to get the absolute travel time for each point. Figure 4 shows the absolute travel time isochrone map developed for basins 1, 2, and 3.

Input to the runoff model was in the form of melt calculated for each grid point on the surface of Burroughs Glacier. This data was applied to both the lumped and distributed lagging routines. Figure 5 represents the hydrographs produced for basins 1,2, and 3 by the lumped method. Figure 6 represents the lagged hydrographs for basins 1, 2, and 3 by the distributed method. Upon close inspection, there does not appear to be any significant difference between output from the two methods. This is further supported by a near one-to-one relationship in a plot of lumped vs distributed lagged outflow for each subbasin shown in figure 7. These lagged hydrographs served as input to the routing routine. Figure 8 compares the lagged-and-routed hydrographs with actual stream hydrographs for basins 1, 2, and 3.

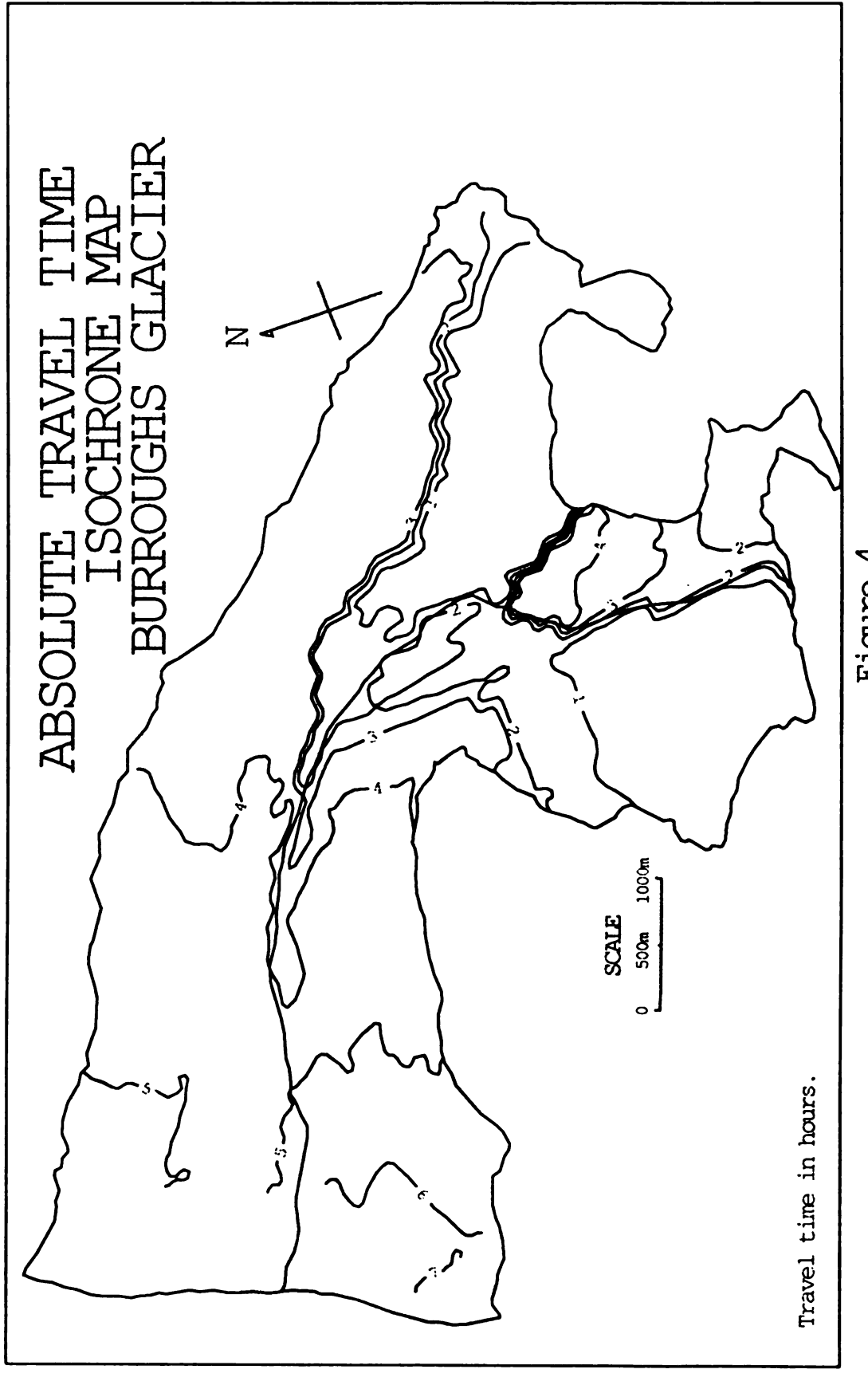
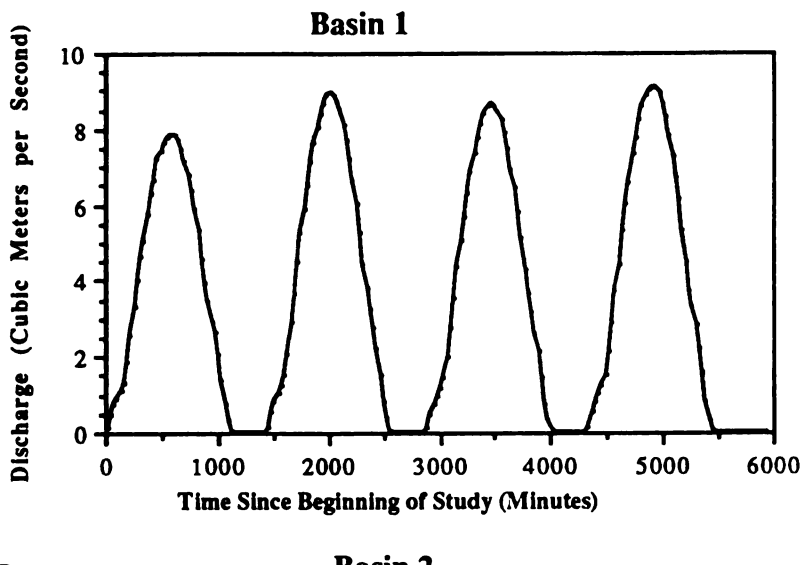
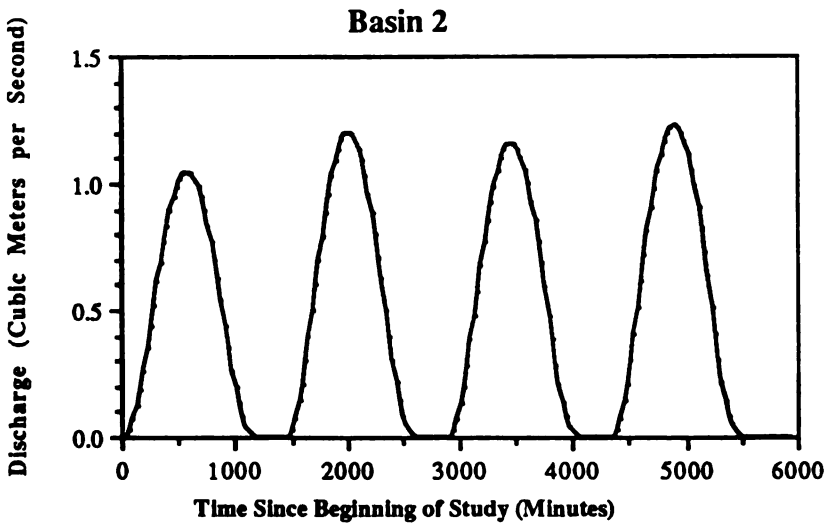


Figure 4





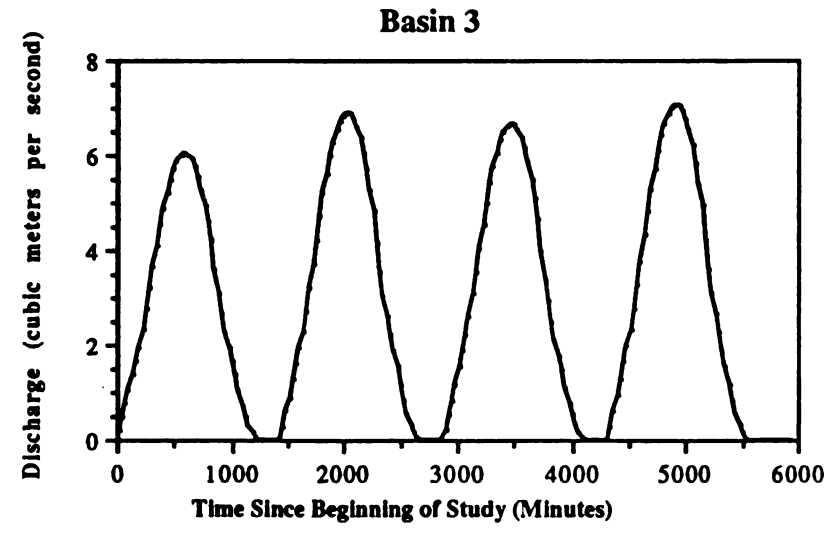


Figure 5. Lumped Model Lagged Hydrographs

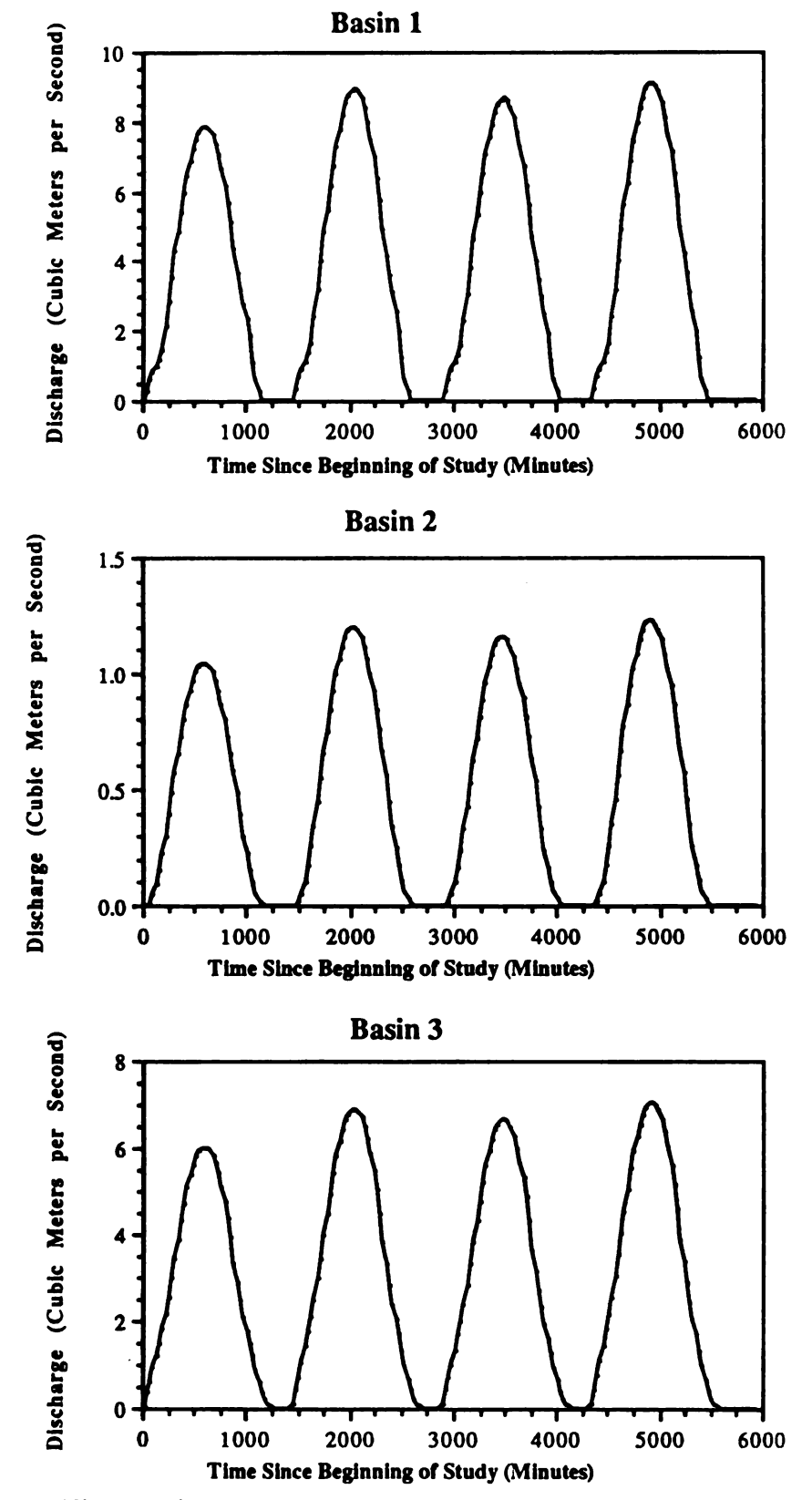


Figure 6. Distributed Model Lagged Hydrographs

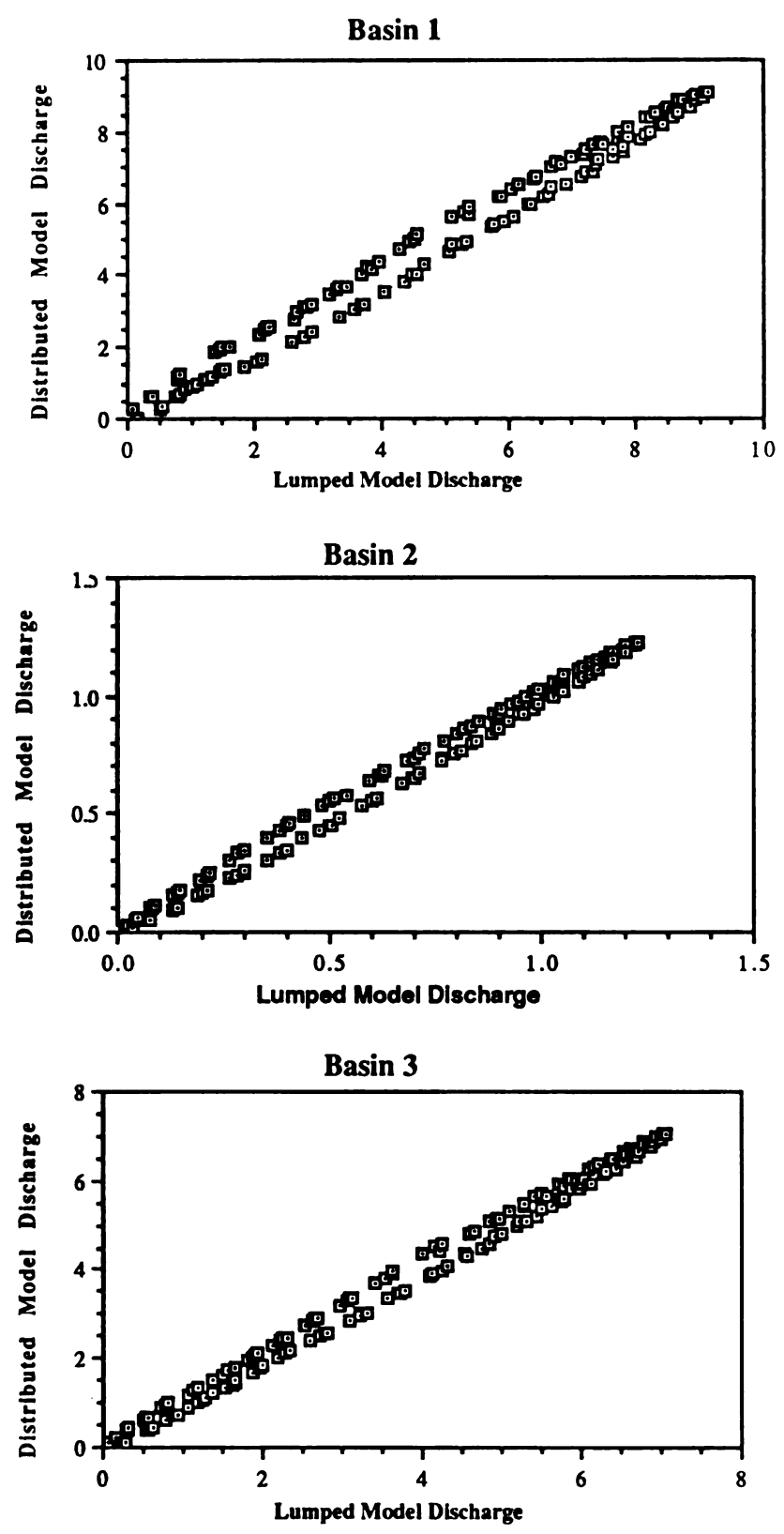


Figure 7. Lumped vs. Distributed Model Outputs

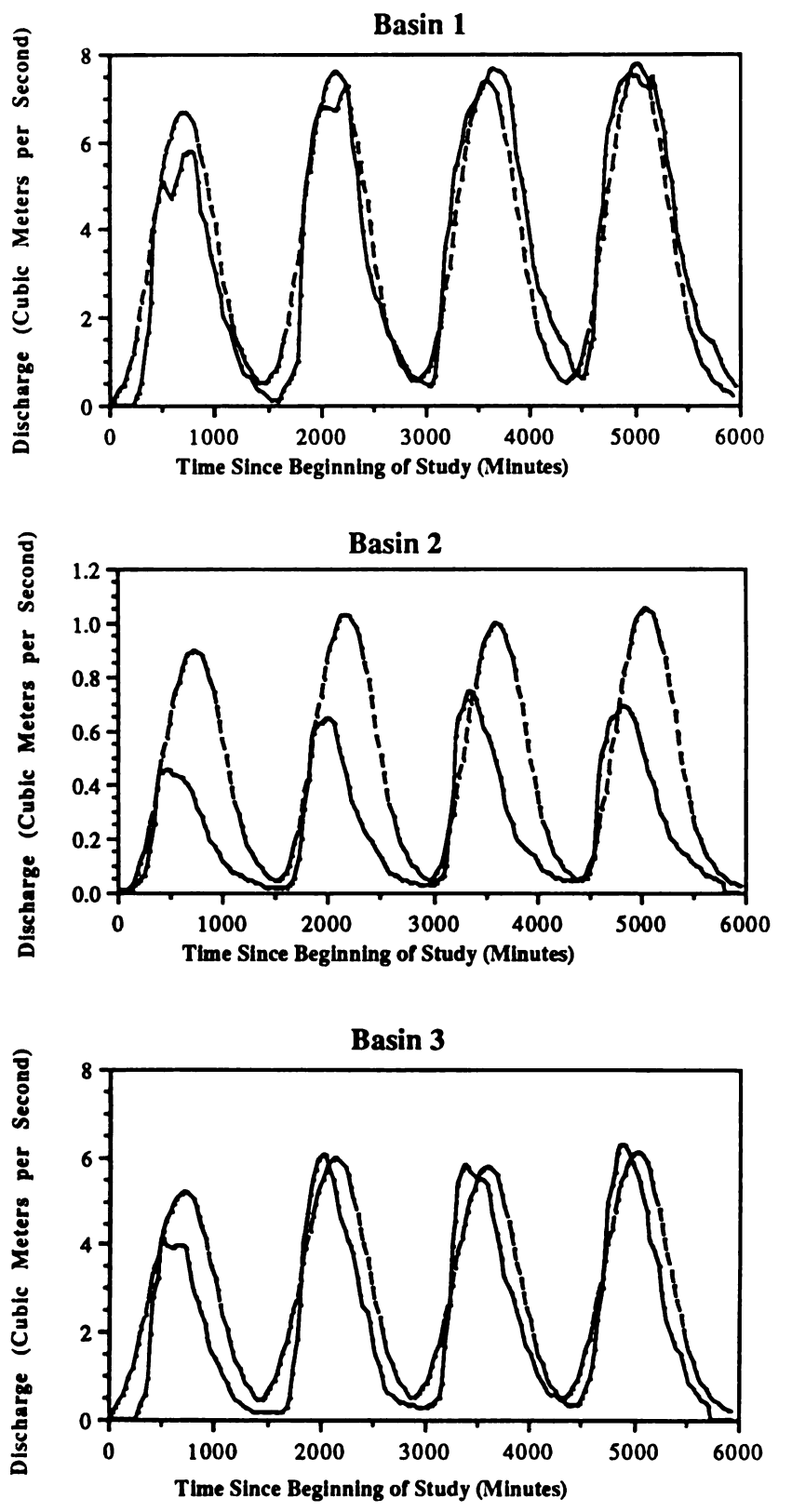


Figure 8. Routed Hydrographs vs. Actual Hydrographs (solid lines=actual flow; dashed lines=modeled flow)

V. RESULTS

Figure 8 shows actual stream discharge and theoretical discharge plotted over the duration of the study period for each of the three subbasins of Burroughs glacier. To measure the ability of the Lag-and-Route model to predict stream discharge, a visual comparison of output discharge and actual discharge was made. Such features as peak discharge, total discharge volume, and time to peak were used as key points of comparison - to determine the degree of correlation for the hydrographs.

From a visual inspection of Figure 8, the model hydrographs and actual stream discharge hydrographs for basins 1 and 3 seem very similar. The model produces peak discharges very close to observed peaks for the two basins - except for the first day. Likewise, total model flow volumes compare favorably with actual flow volumes - with a difference of only 1.91% for basin 1 (see table 4). The simulated discharge for basin 1 also appears to match observed discharge in the time of peak flow. On the other hand, the simulated discharge for basin 3 shows a time of peak arriving slightly after the observed peak flow time (about 3 hours after). Also, on the first day, the observed discharge for basins 1 and 3 appear truncated. Despite these differences, model discharge and simulated discharge are remarkably similar

for basins 1 and 3.

Table 4. Total Stream Discharge during the Study

Basin Number	Actual Volume Discharge	Modeled Volume Discharge	Absolute Difference	Percent Difference	
1	1215626	1238862	23236	1.91	
2	86665	162923	76259	87.99	
3	788952	1013864	224912	28.51	

Moreover, major differences between simulated and observed stream flow, for basins 1 and 3, can be explained. For instance, the apparent difference in basin lag (time of peak flow) between the Lag-and-Route model and actual flow for basin 3 can be explained in terms of a "short-circuit" of the drainage system. Drainage paths on the surface of the glacier were assumed to parallel surface slope (see figure 3). Marginal channels collected drainage from surface flow directed to the side of the glacier and ultimately discharged a total flow at each subbasin outlet. However, it was observed, from aerial photographs, that a submarginal chute existed about two thirds of the way down along the glacier margin from the ice divide. This chute served to divert water flow - so that it could flow straight to the stream outlet. This would tend to decrease the average flow time for water draining from the surface of basin 3 - explaining the earlier time of peak flow for actual stream discharge.

Likewise, the difference in peak discharge between the simulated flow and observed flow on the first day, for basins 1 and

3, can also be explained. The truncation of the actual discharge hydrograph for that day is probably a result of some ephemeral variation in atmospheric conditions. Larson (1978) noted that the afternoon of the first day of the study was somewhat cloudy and hazy - a temporary period of cloudiness, or fog, could account for a sharp drop in radiation input to the glacial surface. And this variation in radiation receipts could explain the variation in stream discharge. The calculated discharge would not show this variation because certain key atmospheric variables used in the melt model were daily averages.

Unlike basin 1 and 3, simulated discharge for basin 2 differs drastically from the observed discharge. Modeled peak flow values for the basin are generally only two thirds the value for actual peak flows. Also, total model flow volumes are only about one half that for actual flow volumes for the basin. And the times of peak flow for the model arrive around 4 hours sooner than the actual peak flows.

Yet, if basin characteristics are taken into account, the results for basin 2 can be explained. Basin 2 is composed chiefly of fractured, and highly weathered, ice. The ice in this zone consists of loose ice crystals in a slushy matrix. This is a highly porous and permeable environment. So much of the water generated at the surface is absorbed into the body of the glacier. Basins 1 and 3, on the other hand, consist of clean (unweathered) ice with no porous covering of snow or detrital material and are characterized as impermeable environments. Relatively little of the

meltwater generated at the surface in such environments would be lost to infiltration.

In summation, discharge generated from the Lag-and-Route model appears to be a good approximation for stream discharge draining basins 1 and 3. Model discharge for basin 1 is a very good match of actual stream flow for the points of comparison (peak flow, flow volume, and time of peak flow). Model peak flow, and flow volume, were also very close to actual values for basin 3. One point of difference between model discharge and actual discharge, for basin 3, was time of peak flow - and that could be explained as a result of an irregularity in the basin.

VI. Conclusions

The lag-and-route method is a surface runoff model.

Stream discharge calculated, using this model, is composed purely of runoff. Observed stream discharge, from subbasins 1 and 3, is equivalent to the discharge produced by the lag-and-route model. Therefore, stream flow from basins 1 and 3 must be wholly a result of surface runoff. If it is further noted that basins 1 and 3 are composed of clean (unweathered) glacial ice, and that meltwater drainage from basins 1 and 3 is accomplished by surface runoff, then it should be accurate to say that meltwater drainage from clean glacial ice must occur through surface runoff. In other words, surface runoff is the major mechanism driving meltwater drainage from unweathered glacial ice.

A knowledge of this mechanism is of importance in many different ways. Natural resources in "marginal" areas will have to be utilized to meet the needs of growing human populations. Some knowledge of glacial hydrologic characteristics will be necessary as human settlement begins to invade glaciated regions. For example, hydrologists must be able to predict the probability, and magnitude, of flooding so that planners/developers/engineers can determine the feasibility of site construction. In glaciated basins, a knowledge of

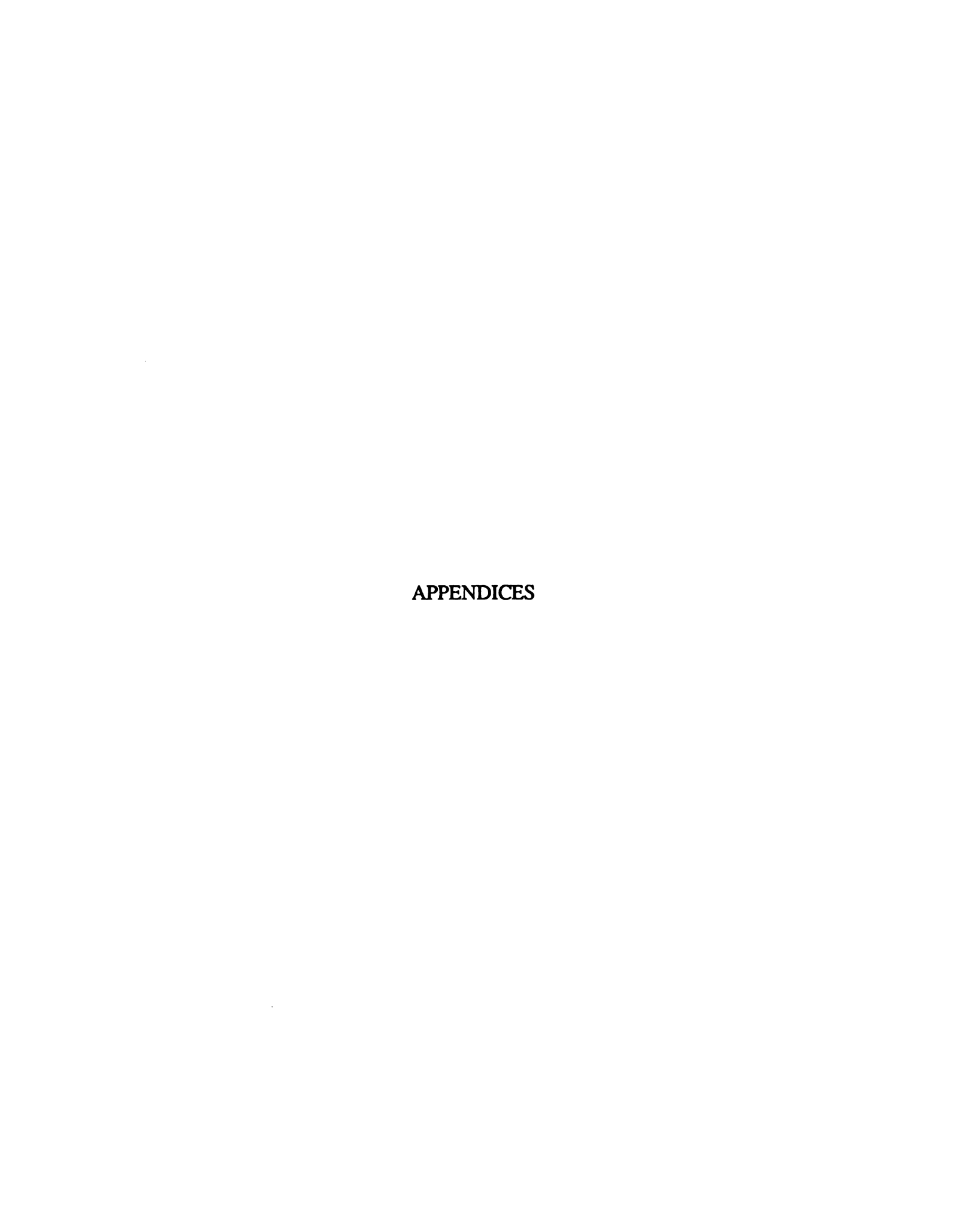
how water drains from glacial ice, and how to model that drainage, would be indispensable in flood prediction.

Another area in which glaciated basins are being exploited is in energy production. Hydroelectric projects are being implemented to take advantage of the tremendous amount of meltwater generated within some glaciated basins. These projects require a detailed analysis of discharge volume, and variation through time, before a site can even be considered. As before, only with a good model of glacial meltwater drainage can a planner truly take the best advantage of the resources available to him. The lag-and-route model, as presented in this study, provides a good approximation.

Surface runoff models, such as the lag-and-route method, can be applied to many different problems concerning glacial hydrology. The lag-and-route model could be used to calculate total daily, and seasonal, flow volumes - which could be used for sizing a reservoir, turbine, and/or generator for a potential hydroelectric site. This model could also be used to show daily, or seasonal, variation in discharge rate, for a specified glacier, so that the manager of a hydroelectric site could manipulate reservoir discharge in such a way as to maintain the smallest variation in hydraulic head while meltwater inflow to the hydroelectric reservoir varies.

The lag-and-route model could also be used to determine the condition of glacial ice. Simulated meltwater discharge, for a glacier, could be calculated and compared to observed discharge. If the two hydrographs compare favorably, then it could be inferred that the glacial ice is clean and relatively unweathered; if the hydrographs do not match, then the glacial ice must be somewhat weathered and/or

disintegrated. Similarly, from comparing model and observed hydrographs, for a snow-covered glacier, it should be possible to determine the effects of the snow cover upon meltwater drainage. However, additional work needs to be done in the area of modeling meltwater drainage through snow and firn. Some sort of porous media flow model could be used to determine the hydraulic characteristics of snow.





Appendix A

Ice Melt Calculations

1. Factors Affecting Melt.

- a. Solar Constant. The sun is approximately 150 million km from the earth. Because of its high surface temperatures (about 6000 K), radiant energy released is high (by Stefan's law). The ray paths of solar radiation diverge as they travel away from the sun, so radiation intensity decreases as the inverse of the square of the distance from the sun. The earth intercepts only one two-billionth of the sun's total energy output (Strahler & Strahler, 1979). The average rate of incoming solar shortwave radiation, at the top of the earth's atmosphere, is known as the solar constant and is around 1.94 calories per square centimeter per minute.
- b. Atmospheric Conditions. Radiation received at the earth's surface must first be filtered through the atmosphere. The radiation intensity at the surface depends, a great deal, upon atmospheric conditions. Overcast conditions may cut down on the amount of radiation received at the surface by either reflecting it back out into space or absorbing it.. Atmospheric moisture content, dust content, or CO2 content will also determine the relative amount of radiation received at the surface. The higher the content the greater the radiation absorption within the atmosphere. One measure of this condition is the atmospheric transmissivity.
- c. Lattitude. Shortwave radiation intensity varies inversely with lattitude with upper lattitudes receiving the least amount of

radiation. Assuming a planar wave front, ray paths are perpendicular to the surface near the equator while the angle of incidence decreases with lattitude. The area over which the radiation between two rays is incident is greater as the angle of incidence increases. The same amount of radiation is expended over a larger area, with greater lattitude, so the intensity decreases.

d. Time of Day. Radiation intensity increases from dawn to solar noon and then decreases from solar noon to dusk. The shortwave angle of incidence is relatively low early and late in the day. This angle is greatest at solar noon, when the area between rays is least and the radiation intensity is greatest. Radiation intensity would then vary as the cosine of the hour angle (which is 90 degrees at solar noon and 0 degrees at dawn and dusk). Times for dawn, solar noon, and dusk varied relatively little during the study period so one value for each was used for the entire period. Expressed in minutes from midnight, the value for dawn, solar noon, and dusk were: 450; 870; and, 1290. From these values, an hour angle can be calculated for any time between dawn and dusk using a simple linear equation.

Hourang = abs((noon-time)/(noon-dawn))*90)

e. Day of Year. Because the earth's axis of rotation is tilted, the point where solar shortwave radiation rays intercepts the earth's surfact at right angles will vary according to which hemisphere is titlted towards the sun. The solar declination is the lattitude angle at which the solar rays impinge perpendicular to the earth's surface (Kondratyev, 1969). For the northern hemisphere, the maximum

solar declination occurs during the summer solstice (June 21) and the minimum occurs during the winter solstice (December 22).

Therefore, radiation intensity increases with increasing declination for the northern hemishpere, and it decreases with decreasing solar declination for the southern hemisphere. Calculations were made for both solar declination and radius vector of the earth's orbit for the four days of the study.

f. Surface Slope/Azimuth. Surface slope and orientation has a great deal of influence upon the amount of shortwave radiation received upon that surface. Obviously, a southerly slope would receive much more solar radiation than a northerly facing slope. Also, the angle of the slope with respect to the incoming solar rays will also have an effect - a surface more perpendicular to these rays will receive a greater radiation intensity. Some term must be included into the generalized law of radiation transmission ($I_d = p^m$). This term (Garnier and Ohmura, 1968; Williams, Barry & Andrews, 1972) may be defined as a complex function of lattitude (phi, hour angle (H), azimuth (A), zenith angle (zx), and declination (delta) - and is expressed as the angle between the sloping surface and the incoming ray vectors (XS).

cos(XS)=((sin(phi)cos(H))(-cos(A)sin(zx)) - sin(H)(sin(A)sin(zx))

- + (cos(phi)cos(H))cos(zx))cos(delta)
- $+(\cos(phi)(\cos(A)\sin(zx))$
- + sin(phi)cos(zx))sin(delta)

The cosine of the angle XS is mutiplied by the radiation transmission equation to get the radiation received on the sloping surface.

g. Surface Albedo. Albedo is a measure of the percentage of radiation that is reflected back off of the surface upon which it is received. Rosenberg (1974), Kondratyev (1969), and many others, have described and measured the reflective abilities of many different materials. Bolsenga (1978) described the variation in reflectivity of ice throughout the day and noticed that there was less than a ten percent variation. The amount of radiation actually absorbed at the surface is calculated as the amount left over after reflectance (1 - albedo).

2. Melt Equations

a. Direct Solar Radiation. Direct solar radiation is that which falls directly on the earth's surface without being diffused through or being reflected off of something else. This may be approximated by an equation developed by Garnier and Ohmura (1968), transformed by Williams, Barry, and Andrews (1972), and applied by Larson (1978). The equation has the form:

$$I_h = \frac{I_o}{r^2} \sum_{k=1}^{n} p^{mk} f(H_k) H$$

Where:

I_o= solar constant = 1.94 cal/cm/min

r = radius vector of the earth's orbit

p = mean-zenith-path transmissivity

m = optical air mass

H = time step

$$f(H_k) = C4\cos(H-Y) + C3$$

 H_k = hour angle measured from solar noon

Y = arctan(C1/C2)

 $C1 = \sin A \sin(q) \cos(delta)$

 $C2 = (\cos(f)\cos(q) - \sin(f)\cos(A)\sin(q))$

 $C3 = (\sin(f)\cos(q) + \cos(f)\cos(A)\sin(q))\sin(d)$

$$C4 = (C1**2 + C2**2)**0.5$$

A = slope azimuth

q = theta = slope angle

f = lattitude

d = declination of the sun

Here, I_h stands for the hourly total radiation input to the surface.

b. Diffuse Radiation. Diffuse radiation consists of that radiation incident to a surface originating from radiation scattered in the atmosphere. Diffuse radiation is that portion of the radiation that permeates a surface when it is shaded from direct sunlight. Equations were also developed (List, 1966; Garnier and Ohmura, 1968; Williams et al, 1972) to approximate diffuse radiation inputs. This equation has the form:

$$D_0 = 0.5 \frac{I_0}{r^2} \sum_{k=1}^{n} (0.91 - p^{mk}) \cos(Z_s) H$$

where:

 Z_s = zenith angle

 I_0 = solar constant = 1.94 cal/cm/min

r = radius vector of the earth's orbit

p = mean-zenith-path transmissivity

m = optical air mass

H = time step

 $cos(Z_s) = cos(dx)cos(fx)cos(H) + sin(dx)sin(f)$

H = hour angle measured from solar noon

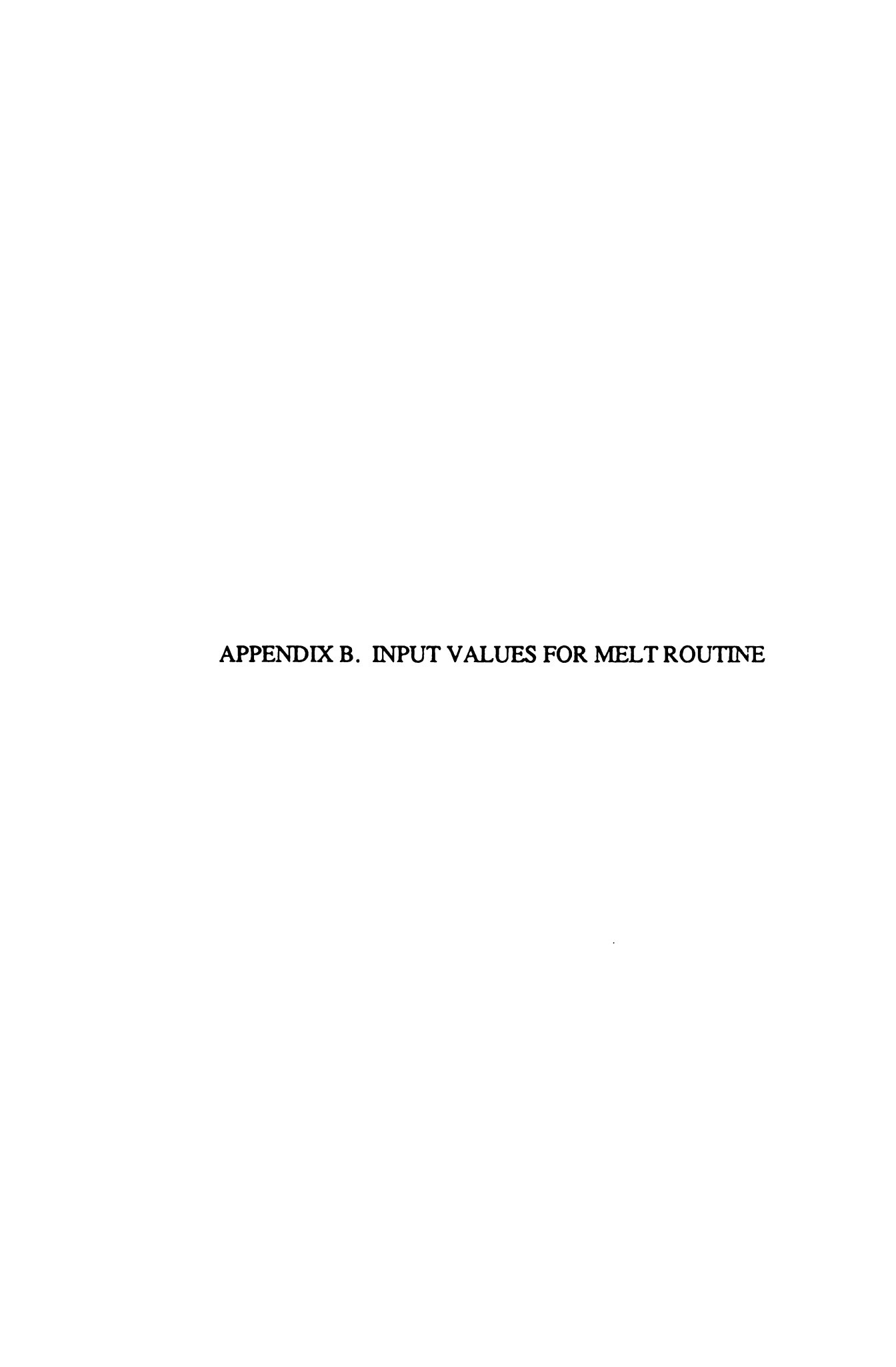
f = lattitude

d = declination of the sun

The variables for this equation are the same as for the previous except for the zenith angle. Here, too, the time interval chosen was 30 minutes for the hourly diffuse radiation inputs to the surface.

c. Total Radiation at Surface. The total shortwave radiation received at the earth's surface is the sum of the direct and diffuse radiation inputs. The amount actually gained by the surface of the glacial ice is this sum of shortwave radiation minus that percentage that is reflected back up to the atmosphere. Given a reflectivity value (r), the total radiation gain would be the total incident radiation multiplied by the absorptivity (a=1-r).

Igain = It =
$$(I_h - D_o)(1-r)$$



APPENDIX B

Input Values for Melt Routine

The melt program requires the use of two different kinds of data: data that changes value temporily; and, data that changes value areally.

Certain input data pertain to every point on the glacial surface but not to every day of the study period (they vary in value from one day to the next) - these variables include: atmospheric transmissivity; declination; and, radius vector. Table B.1 displays the values for these variables for the four days of the study.

Table 5

Daily Variable Data Values

Variable\Day	11	2	3	44	_
atmospheric transmissivity	0.51	0.67	0.64	0.71	
solar declination	14.6085	14.30	13.9915	13.6830	
radius vector	1.012995	1.012810	1.012625	1.012440	

Referring to the grid system for the glacier, slope and slope azimuth was calculated for each point on the grid. This was done by statistically fitting a linear regression plane through every set of nine points in a three by three matrix. At some points, which lay along the margin of the glacier, the slope and slope azimuth were approximated by fitting a plane to the point in question and any two or more adjacent points on the ice. Figures B.1 and B.2 show the variation of slope and slope azimuth over the surface of Burroughs Glacier.

The reflectivity (or albedo) of the glacier surface was measured during the early afternoon of August 15, 1973 by G. Larson. Total incoming solar radiation was measured at each of 17 points at the ice surface using an horizontally mounted Eppley pyranometer. Reflected radiation was measured at each of these stations by inverting the pyranometer and taking measurements. The albedo was calculated for each point by dividing the amount of reflected radiation by the amount of total incoming radiation. Albedo variation over the glacier surface could then be determined by assuming a linear variation between each pair of points on the surface. Figure B.3 shows this variation in albedo for the glacier.

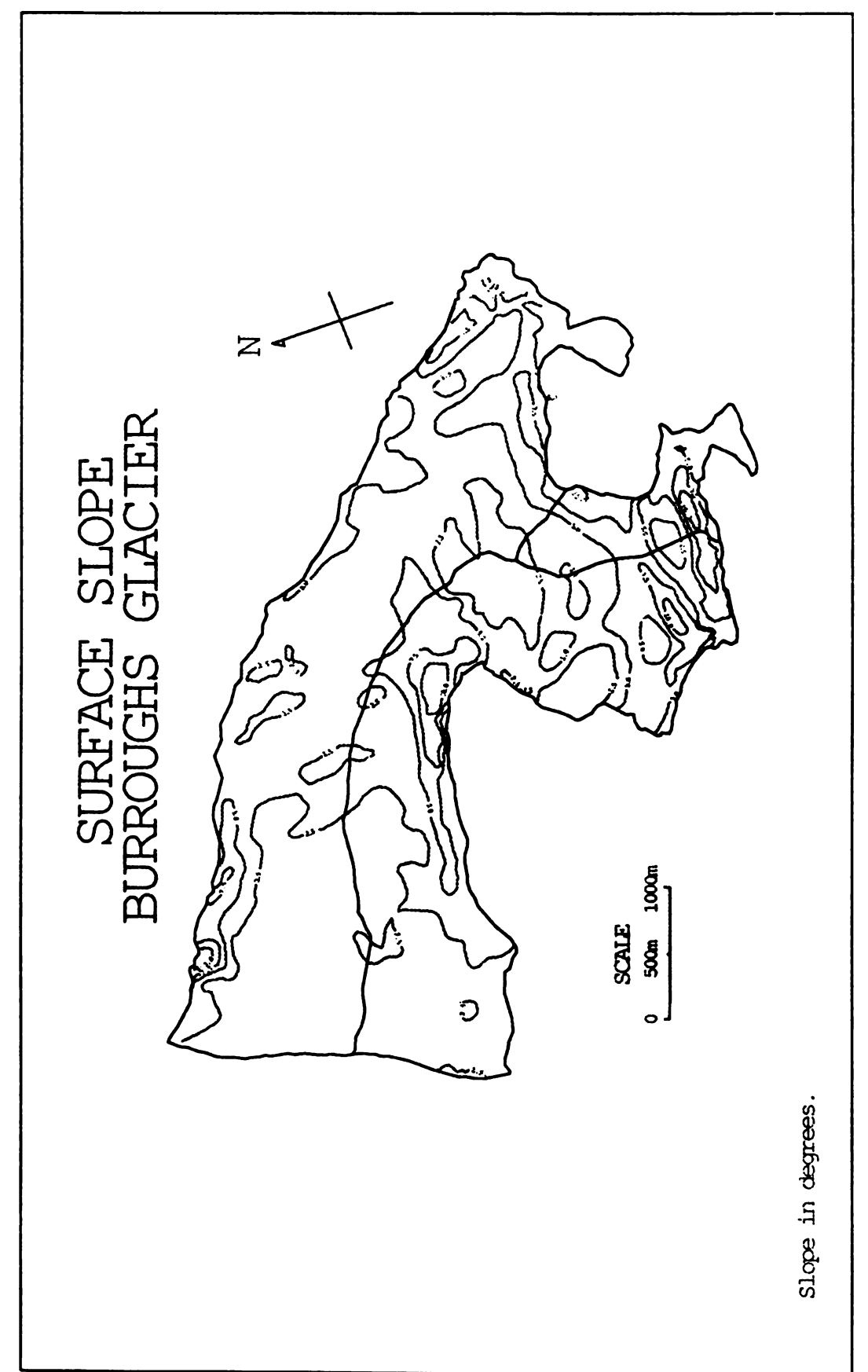


Figure 9

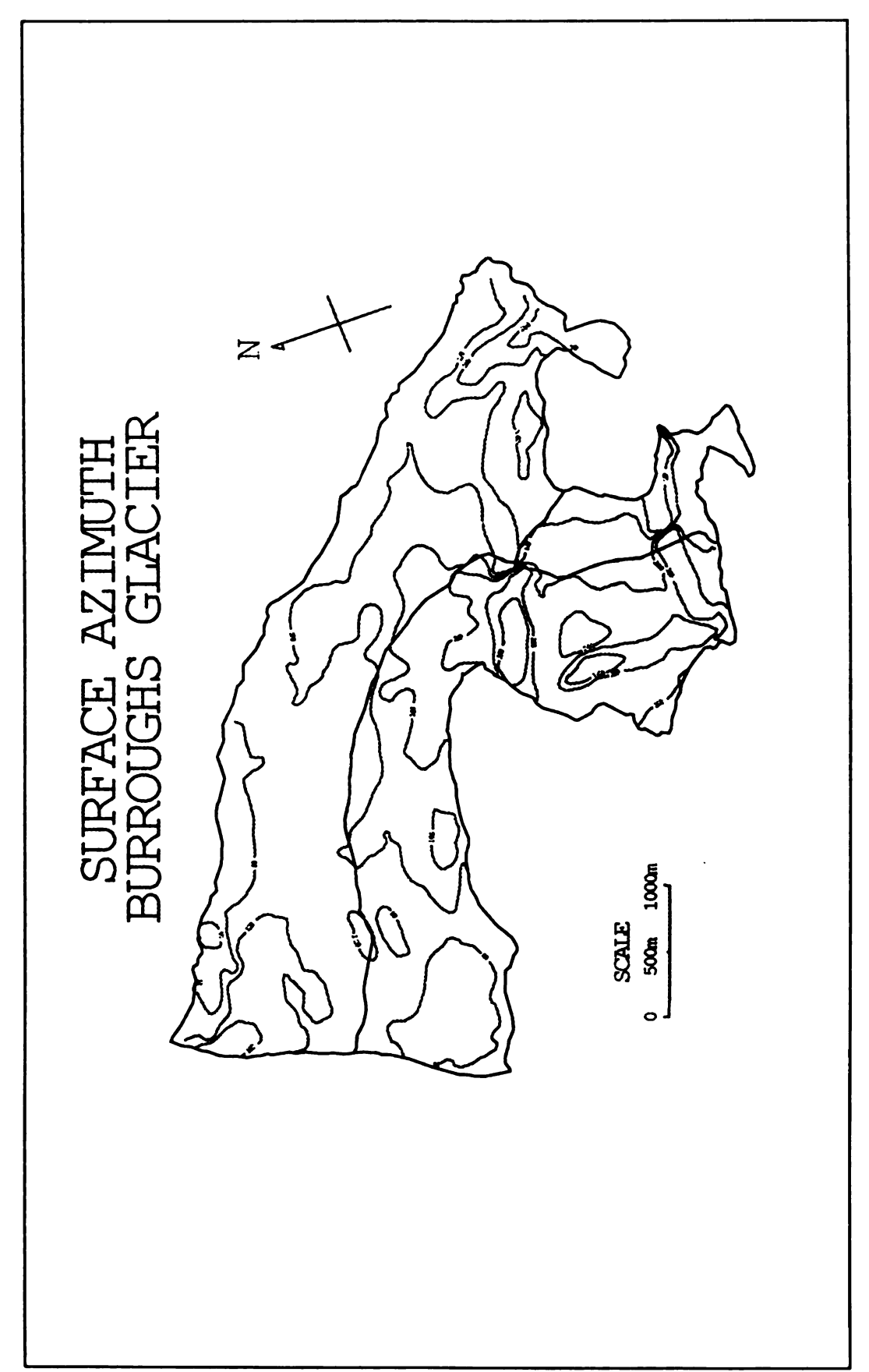


Figure 10

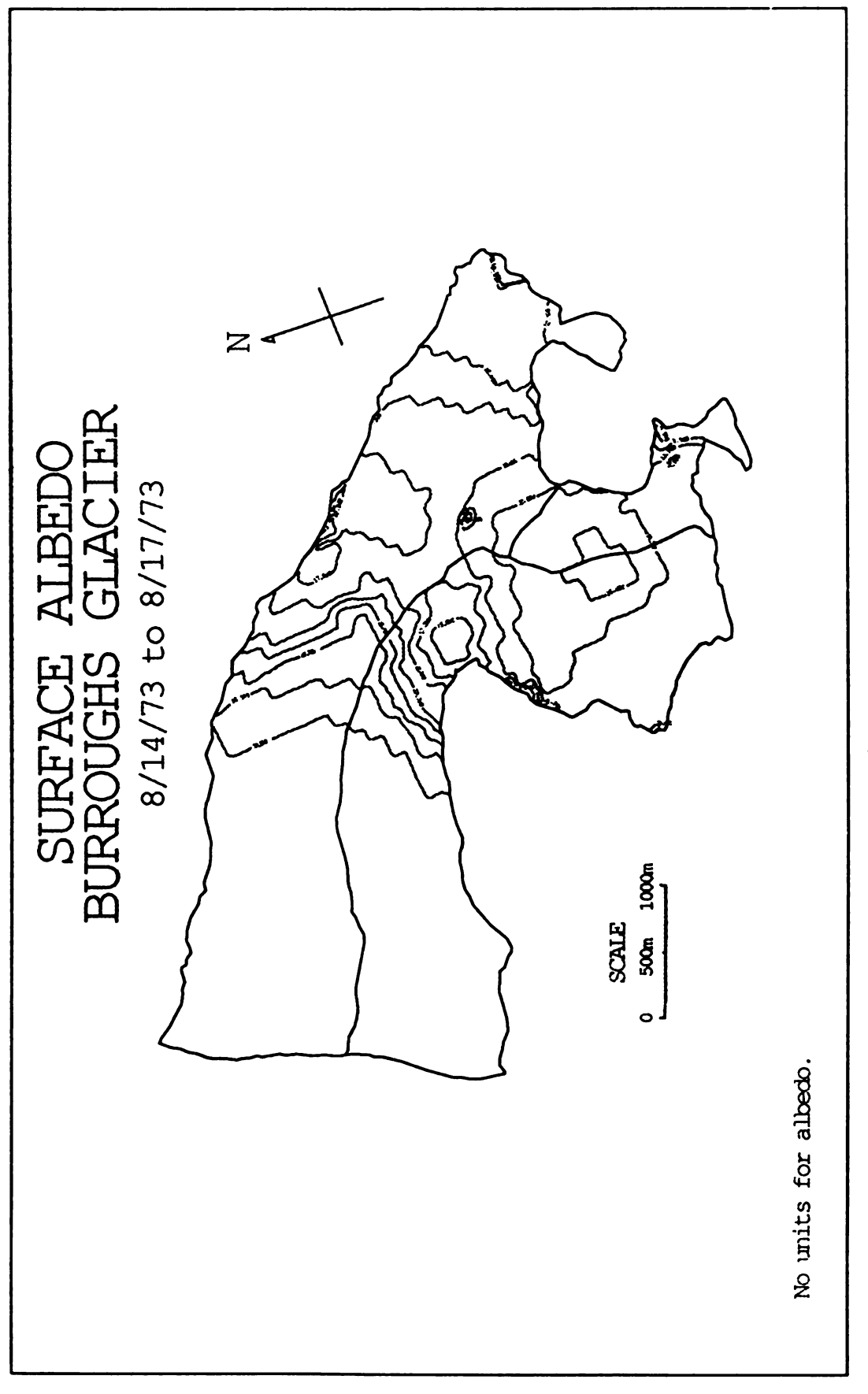


Figure 11



APPENDIX C

Program to Calculate Hour Angles

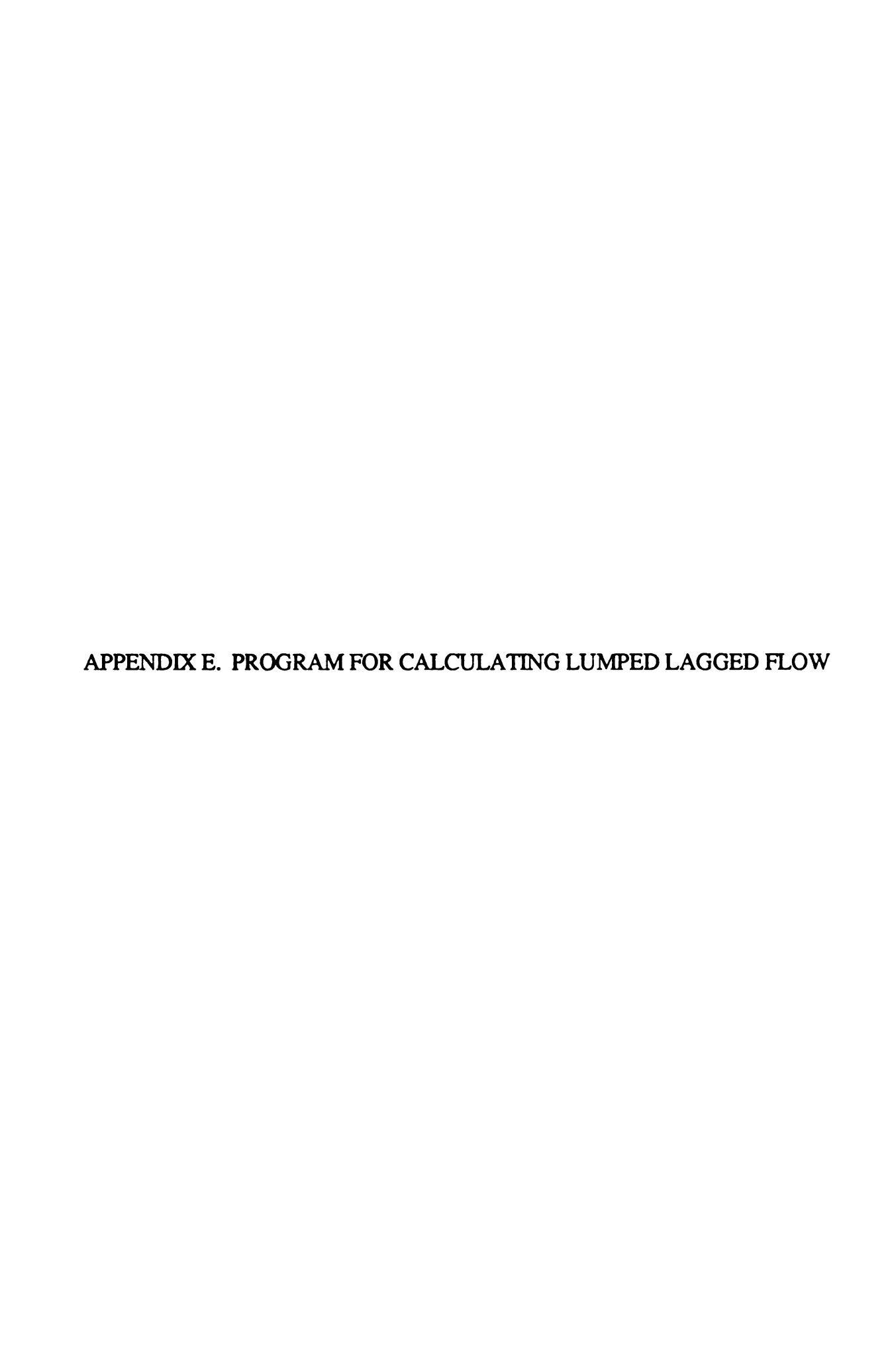
```
data hangle;
  dawn=450;
  dusk=1290;
  noon=870;
  conrad=0.0174532;
  do tim=465 to 1275 by 30;
     hrang=abs(((noon-tim)/(noon-dawn))*90);
     hrang=hrang*conrad;
  output;
  end;
proc print data=hangle;
run;
```



APPENDIX D

Program to Calculate Radiation Receipts and Melt

```
CMS FILEDEF INDATA DISK RAW1 DAT A;
CMS FILEDEF OUTDATA DISK ML1RD45 DAT A:
data melrad (keep=x y gridrad gridmel);
 infile indata:
 input x y slope az albedo;
 file outdata;
 HOURANG=1.06589;
  conrad=0.0174532;
  AR=1.012440;
 PE=0.710:
DEC=13.6830*CONRAD;
  lat=58.9666*conrad;
  slope=slope*conrad;
 az=az*conrad;
 solcon=1.94:
 tint=30:
  gridrad=0.0:
   opairms=1.0/(cos(dec)*cos(lat)*cos(hourang)+sin(dec)*sin(lat));
 if opairms le 0.0 then go to flag1;
  c1=-sin(az)*sin(slope)*cos(dec);
  c2=(cos(lat)*cos(slope)-sin(lat)*cos(az)*sin(slope))*cos(dec);
  c3=(sin(lat)*cos(slope)+cos(lat)*cos(az)*sin(slope))*sin(dec);
 c5=c1/c2:
  y2=atan(c5);
  c4 = sqrt(c1**2+c2**2);
  fh=c4*cos(hourang-y2)+c3;
  cosz=1/opairms;
  ir=(solcon/ar**2)*fh*tint*(pe**opairms);
   d=0.5*(0.91pe**opairms)*cosz*tint*((cos(slope/2.0))**2)
     *solcon/(ar**2);
 if fh le 0.0 then go to flag1;
   gridrad = ((100-albedo)/100)*(ir+d);
  flag1: gridmel=gridrad/79.720;
  put x 1-5 y 6-10 gridrad 11-20 .5 gridmel 21-30 .6;
run;
```



APPENDIX E

Program to Calculate Lumped Lagged Flow

```
CMS FILEDEF INDATA DISK ML3RD414 DAT A1:
CMS FILEDEF OUTDATA DISK FLO3414 DAT A1:
DATA ONE (KEEP=X Y RAD MEL):
 RETAIN FLAG 0:
 do:
 infile indata:
 INPUT X 1-5 Y 6-10 RAD 11-20 MEL 21-30;
 IF NOT((X EQ 6 AND Y EQ 24) OR (X EQ 7 AND (Y EQ 22 OR Y EQ 23
  OR Y EO 24)) OR (X EO 8 AND (Y EO 20 OR Y EO 23 OR Y EO 24))
  OR (X EO 9 AND (Y EO 24 OR Y EO 25)) OR (X EO 10 AND
  Y EQ 18) OR (X EQ 11 AND (Y EQ 17 OR Y EQ 18)) OR
  (X EQ 12 AND (Y EQ 15 OR Y EQ 16 OR Y EQ 17 OR Y EQ 18))
  OR (X EO 13 AND (Y EO 15 OR Y EO 16 OR Y EO 17 OR Y EO 18))
  OR (X EO 14 AND (Y EO 16 OR Y EO 17 OR Y EO 18)) OR
  (X EQ 15 AND (Y EQ 17 OR Y EQ 18)) OR (X EQ 16 AND
  (Y EQ 17 OR Y EQ 18)) OR (X EQ 29 AND Y EQ 50) OR
  (X EQ 39 AND Y EQ 29)) THEN DO:
   IF X EO 37 AND Y EO 38 AND FLAG EO 0 THEN DO:
     FLAG+1:
     X=34;
   END:
   OUTPUT;
 END:
 end;
run:
CMS FILEDEF INDATA DISK ABSTIM3 DAT A1:
data two;
 do:
  infile indata;
  input x 1-5 y 6-10 reltim 11-20 abstim 21-30;
 end:
run:
PROC SORT DATA=ONE:
BY X Y;
RUN:
PROC SORT DATA=TWO:
BY X Y:
```

```
RUN:
data three:
 do:
 merge one two;
BY X Y:
 end:
run:
DATA FOUR;
 set three;
 RETAIN AREA05 AREA10 AREA15 AREA20 AREA25 AREA30
  AREA35 AREA40 AREA45 AREA50 AREA55 AREA60 AREA65
  AREA70 AREA75 FLOW05 FLOW10 FLOW15 FLOW20 FLOW25
  FLOW30 FLOW35 FLOW40 FLOW45 FLOW50 FLOW55 FLOW60
  FLOW65 FLOW70 FLOW75 COUNT05 COUNT10 COUNT15 COUNT20
  COUNT25 COUNT30 COUNT35 COUNT40 COUNT45 COUNT50
  COUNT55 COUNT60 COUNT65 COUNT70 COUNT75 FLAG 0.0;
 do:
 flag+1:
 IF (ABSTIM GT 7.0) AND (ABSTIM LE 7.5) THEN DO;
 COUNT75=COUNT75+1:
  AREA75=AREA75+MEL;
  end:
  else
  IF (ABSTIM GT 6.5) AND (ABSTIM LE 7.0) THEN DO:
  COUNT70=COUNT70+1:
  AREA70=AREA70+MEL:
   end:
  else
  IF (ABSTIM GT 6.0) AND (ABSTIM LE 6.5) THEN DO:
   COUNT65=COUNT65+1:
   AREA65=AREA65+MEL:
   end:
   else
   IF (ABSTIM GT 5.5) AND (ABSTIM LE 6.0) THEN DO;
   COUNT60=COUNT60+1:
    AREA60=AREA60+MEL:
    end;
   else
    IF (ABSTIM GT 5.0) AND (ABSTIM LE 5.5) THEN DO;
    COUNT55=COUNT55+1:
    AREA55=AREA55+MEL:
    end:
    else
```

```
IF (ABSTIM GT 4.5) AND (ABSTIM LE 5.0) THEN DO;
COUNT50=COUNT50+1;
AREA50=AREA50+MEL;
end:
else
 IF (ABSTIM GT 4.0) AND (ABSTIM LE 4.5) THEN DO;
 COUNT45=COUNT45+1;
 AREA45=AREA45+MEL:
  end:
 else
  IF (ABSTIM GT 3.5) AND (ABSTIM LE 4.0) THEN DO;
  COUNT40=COUNT40+1:
  AREA40=AREA40+MEL:
  END:
 ELSE
  IF (ABSTIM GT 3.0) AND (ABSTIM LE 3.5) THEN DO;
  COUNT35=COUNT35+1:
   AREA35=AREA35+MEL:
  END:
  ELSE
   IF (ABSTIM GT 2.5) AND (ABSTIM LE 3.0) THEN DO:
   COUNT30=COUNT30+1:
   AREA30=AREA30+MEL:
   END:
   ELSE
    IF (ABSTIM GT 2.0) AND (ABSTIM LE 2.5) THEN DO:
    COUNT25=COUNT25+1;
    AREA25=AREA25+MEL:
   END;
   ELSE
    IF (ABSTIM GT 1.5) AND (ABSTIM LE 2.0) THEN DO:
    COUNT20=COUNT20+1:
    AREA20=AREA20+MEL;
    END:
    ELSE
     IF (ABSTIM GT 1.0) AND (ABSTIM LE 1.5) THEN DO;
    COUNT15=COUNT15+1:
     AREA15=AREA15+MEL;
    END:
    ELSE
     IF (ABSTIM GT 0.5) AND (ABSTIM LE 1.0) THEN DO;
     COUNT10=COUNT10+1;
      AREA10=AREA10+MEL:
```

```
END:
          ELSE
           DO:
           COUNT05=COUNT05+1:
            AREA05=AREA05+MEL:
           END:
 IF FLAG EQ 489 THEN DO:
  flow75 = ((area75/count75)/100.0)*(count75*10000.0)/1800.0;
  flow70 = ((area70/count70)/100.0)*(count70*10000.0)/1800.0
  flow65 = ((area65/count65)/100.0)*(count65*10000.0)/1800.0;
  flow60 = ((area60/count60)/100.0)*(count60*10000.0)/1800.0;
  flow55 = ((area55/count55)/100.0)*(count55*10000.0)/1800.0;
  flow50 = ((area50/count50)/100.0)*(count50*10000.0)/1800.0
  flow45 = ((area45/count45)/100.0)*(count45*10000.0)/1800.0;
  flow40 = ((area40/count40)/100.0)*(count40*10000.0)/1800.0;
  flow35=((area35/count35)/100.0)*(count35*10000.0)/1800.0;
  flow30 = ((area30/count30)/100.0)*(count30*10000.0)/1800.0;
  flow25 = ((area25/count25)/100.0)*(count25*10000.0)/1800.0;
      flow 20 = ((area 20/count 20)/100.0)*(count 20*10000.0)/1800.0;
      flow 15 = ((area 15/count 15)/100.0)*(count 15*10000.0)/1800.0:
  flow10=((area10/count10)/100.0)*(count10*10000.0)/1800.0;
  flow05 = ((area05/count05)/100.0)*(count05*10000.0)/1800.0;
   file outdata:
   PUT FLOW75 1-10 .6;
   PUT FLOW70 1-10 .6:
   PUT FLOW65 1-10 .6:
   PUT FLOW60 1-10 .6:
   PUT FLOW55 1-10 .6:
   PUT FLOW50 1-10 .6:
   PUT FLOW45 1-10 .6:
   PUT FLOW40 1-10 .6:
   PUT FLOW35 1-10 .6;
   PUT FLOW30 1-10 .6:
   PUT FLOW25 1-10 .6:
   PUT FLOW20 1-10 .6:
   PUT FLOW15 1-10 .6:
   PUT FLOW10 1-10 .6:
   PUT FLOW05 1-10 .6:
 end;
 end;
run;
```

APPENDIX F. PROGRAM FOR CALCULATING DISTRIBUTED LAGGED **FLOW**

APPENDIX F

Program to Calculate Distributed Lagged Flow

```
CMS FILEDEF INDAT2 DISK ABSTIM2 DAT A:
CMS FILEDEF INDAT1 DISK RAW2 DAT A;
CMS FILEDEF OUTDATA DISK ND30FL2 DAT A;
DATA _null_;
DO:
 ARRAY MELT(190) M1-M190;
 RETAIN M1-M190 KOUNT1 0.0:
KOUNT1+1;
  conrad=0.0174532;
 INFILE INDAT1:
INPUT X Y SLOPE AZ ALBEDO;
SLOPE=SLOPE*CONRAD:
AZ=AZ*CONRAD:
 INFILE INDAT2:
 INPUT X Y RELTIM FLOTIM;
 FLOTIM=FLOTIM*2.0;
FLOTIM=ROUND(FLOTIM);
  dawn=450:
  dusk=1290;
  noon=870:
  lat=58.9666*conrad;
 solcon=1.94;
 TINT=30:
 DO DAY=1 TO 4 BY 1;
IF DAY EQ 1 THEN DO:
  ar=1.012995;
 pe=0.510;
  dec=14.6085*conrad;
END:
IF DAY EQ 2 THEN DO;
  AR=1.012810;
 PE=0.670;
DEC=14.30*CONRAD;
END:
IF DAY EQ 3 THEN DO;
  AR=1.012625;
 PE=0.640;
```

```
DEC=13.9915*CONRAD;
END;
IF DAY EQ 4 THEN DO;
 AR=1.012440;
 PE=0.710;
DEC=13.6830*CONRAD;
END:
 DO TIM=465 TO 1275 BY 30;
 HOURANG=ABS(((NOON-TIM)/(NOON-DAWN))*90);
HOURANG=HOURANG*CONRAD;
  gridrad=0.0;
   opairms=1.0/(cos(dec)*cos(lat)*cos(hourang)+sin(dec)*sin(lat));
 if opairms le 0.0 then go to flag1;
 C1=-SIN(AZ)*SIN(SLOPE)*COS(DEC);
 C2=(COS(LAT)*COS(SLOPE)
   -SIN(LAT)*COS(AZ)*SIN(SLOPE))*COS(DEC);
 C3=(SIN(LAT)*COS(SLOPE)
   +COS(LAT)*COS(AZ)*SIN(SLOPE))*SIN(DEC);
  c5=c1/c2:
  y2=atan(c5);
  c4 = sqrt(c1**2+c2**2);
  fh=c4*cos(hourang-y2)+c3;
  cosz=1/opairms;
  ir=(solcon/ar**2)*fh*tint*(pe**opairms);
 D=0.5*(0.91-PE**OPAIRMS)*COSZ*TINT
        *((COS(SLOPE/2.0))**2)*SOLCON/(AR**2);
 if fh le 0.0 then go to flag1:
 GRIDRAD=((100-ALBEDO)/100)*(IR+D);
 FLAG1: GRIDMEL=GRIDRAD/79.720;
  KOUN = (((TIM-465+30)/30) + ((DAY-1)*48)) + FLOTIM;
 MELT(KOUN)=MELT(KOUN)+GRIDMEL*(10000/100)/(1800);
END:
END:
 IF KOUNT1 EQ 73 THEN DO:
 FILE OUTDATA:
 DO KOUN=1 TO 190 BY 1;
  PUT MELT(KOUN) 1-20 .6;
END:
 end;
END;
RUN;
```



APPENDIX G

Program to Calculate Routed Flow

```
CMS FILEDEF INDAT DISK FLO3TOT DAT A;
CMS FILEDEF OUTDAT DISK ROUTFL3 DAT A;
DATA TEMP:
DO;
 ARRAY OUT(199) O1-O199;
 ARRAY IN(199) I1-I199;
 T=0.50:
 K=3.21;
 CO=(0.5*T)/(K+0.5*T);
C1=C0;
 C2=(K-0.5*T)/(K+0.5*T);
 INFILE INDAT:
FILE OUTDAT;
 INPUT IN(1);
 OUT(1)=0.0;
 DO KOUNT=2 TO 199 BY 1;
  INPUT IN(KOUNT);
 OUT(KOUNT)=CO*IN(KOUNT)+C1*IN(KOUNT-1)+C2*OUT(KOUNT-1);
  PUT OUT(KOUNT) 1-20 .6;
END:
END;
```



Bibliography

- Bolsenga, S. J. "Preliminary Observations on the Daily Variation of Ice Albedo", <u>Journal of Glaciology</u>, Vol 18, No 80, pg. 517-521, 1977.
- Bolsenga, S. J. "Solar Altitude Effects on Ice Albedo", NOAA
 Technical Memorandum ERL GLERL-25, Great Lakes
 Environmental Research Laboratory, Ann Arbor,
 Michigan, June 1979.
- Drewry, David "Glacial Geologic Processes", Edward Arnold (Publishers) Ltd., Baltimore, 1986.
- Freeze, R. Allan "Role of Subsurface Flow in Generating Surface Runoff 1. Base Flow Contributions to Channel Flow", Water Resources Research, Vol. 8, No. 3, pg. 609-623, 1972.
- Garnier, B. J. and A. Ohmura "A Method of Calculating the Direct Shortwave Radiation Income of Slopes", <u>Journal of Applied Hydrology</u>, Vol. 7, pg. 796-800, 1968.
- Kondratyev, K. Ya. "Radiation in the Atmosphere", Academic Press, New York, 1969.
- Larson, Grahame J. "Internal Drainage of Stagnant Ice: Burroughs Glacier, Southeast Alaska", Institute of Polar Studies, Report No 65, Ohio State University, Columbus, Ohio, 1977.
- Larson, Grahame J. "Meltwater Storage in a Temperate Glacier Burroughs Glacier, Southeast Alaska", Institute of Polar Studies and Department of Geology and Minerology, Report No 66, Ohio State University, Columbus, Ohio, 1978.

- Laurenson, E. M. "A Catchment Storage Model for Runoff Routing", Journal of Hydrology, Vol. 2, pg. 141-163, 1964.
- Linsley, Ray K., Max A. Kahler, and Joseph L. H. Paulhus "Hydrology for Engineers", 2nd ed, McGraw-Hill, New York, 1975.
- List, R. J., ed "Smithsonian Meteorolgical Tables", 6th ed, Smithsonian Misc. Collections Vol. 114, Smithsonian Institute, Washington, D.C., 1966.
- Loewe, F. "Climate", in Mirsky, A., ed., "Soil Development and Ecological Succession in a Deglaciated Area of Muir Inlet, Southeast Alaska", Ohio State University Institute of Polar Studies, Report 20, pg. 19-28, 1966.
- McKenzie, Garry D. "Glacial History of Adams Inlet, Southeast Alask", Ohio State University, PhD Dissertation, 1968.
- McKenzie, Garry D. "Glacial Geology of Adams Inlet, Southeast Alaska", Institute of Polar Studies, Report No 25, The Ohio State University Research Foundation, Columbus, Ohio, November 1970.
- Mickelson, David M. "Glacial Geology of the Burrough's Glacier Area, Southeast Alaska", Institute of Polar Studies, Report No 40, The Ohio State University Research Foundation, Columbus, Ohio, 1971.
- Nye, J. F. "Water at the Bed of a Glacier", in "Symposium on the Hydrology of Glaciers", Pub. No. 95, pg. 189-194, 1973.
- Nye, J. F. "Water Flow in Glaciers: Jokulhlaups, Tunnels and Veins", Journal of Glaciology, Vol 17, No 76, pg. 181-207, 1976.
- Nye, J. F. and F. C. Frank "Hydrology of the Intergranular Veins in a Temperate Glacier" in "Symposium on the Hydrology of Glaciers", Pub. No. 95, pg. 157-161, 1973.
- Rosenberg, Norman J. "Microclimate: The Biological Environment", John Wiley & Sons, New York, 1974.

MICHIGAN STATE UNIV. LIBRARIES
31293006207298